

***H-T* phase diagram for spin-glasses: An experimental study of Ag:Mn**R. V. Chamberlin, M. Hardiman,\* L. A. Turkevich,<sup>†</sup> and R. Orbach*Department of Physics, University of California at Los Angeles, Los Angeles, California 90024*

(Received 9 November 1981)

We present high-resolution SQUID (superconducting quantum interference device) measurements of the dc magnetization on two Ag:Mn samples containing 2.6 and 4.0 at. % Mn. We have measured in detail the temperature dependence of the magnetization on warming through the glass temperature,  $T_G$ , (i) after cooling to  $T < T_G$  in a near-zero field and then applying the measurement field, zero-field cooled, and (ii) after cooling to  $T < T_G$  in the measurement field. This has been done for fields  $0.5 \leq H \leq 500$  Oe. The temperature derivative,  $dM(H, T)/dT$ , of the ZFC curve shows structure, allowing the identification of several characteristic temperatures associated with the paramagnetic to spin-glass transition in the presence of an external magnetic field. The temperature,  $T_B$ , where the crossover from a Curie-like to a nonlinear susceptibility occurs, behaves as  $\sim H^{0.5 \pm 0.1}$ . Two further temperatures,  $\bar{T}$  and  $T_p$ , where  $\bar{T} < T_p < T_G^0(H \rightarrow 0)$  are suggested as possible candidates for the theoretical-field-dependent transition temperature  $T_G(H)$  given by  $[1 - [T_G(H)/T_G^0]] = Ah^{2/3}$  where  $h = H/J = g\mu_B H/k_B T_G^0$  and  $A$  is of order unity. We find  $[1 - [\bar{T}(H)/T_G^0]] = Bh^{0.70 \pm 0.05}$ , but where  $B$  is approximately  $(19)^{2/3}$ . However, the  $T_p$  data are consistent with the theoretical prediction ( $A \approx 1$ ) using no adjustable parameters, but the range of data is insufficient to enable an unambiguous verification of the theory. On the basis of recent theories, we suggest that the system entering the spin-glass phase at  $T_G(H)$  should be marked experimentally by  $\chi_{dc} = M/H_{static} > \chi_{ac}(\nu, H_{osc}, H_{static})$  where  $M$  is the magnetization,  $H_{static}$  the magnitude of the dc field,  $H_{osc}$  the amplitude of the ac oscillating field, and  $\nu$  its frequency. This argument leads us to conclude that  $T_p(H)$  should be taken as the experimental definition of  $T_G(H)$ .

**I. INTRODUCTION**

Spin-glasses<sup>1</sup> are characterized by the abrupt changes in their low-frequency ac susceptibility and low-field dc magnetization which will occur at a well-defined temperature  $T_G$ . Above  $T_G$ , these materials are paramagnetic. Below  $T_G$ , there is a sharp drop in the ac response with decreasing temperature. The field cooled dc response, however, is approximately temperature independent.<sup>2</sup> Changing the dc field below  $T_G$  leads to a slow, quasilogarithmic time dependence of the dc magnetization.<sup>3</sup> A measurement of the ac or dc response, even in modest fields, produces a severe rounding of the transition.<sup>1</sup>

Much theoretical effort<sup>4</sup> has been devoted to a description of the transition from the paramagnetic to the "frozen" spin-glass state and to the actual nature of the frozen state. The modification of the spin-glass transition by an external magnetic field is now receiving considerable attention. In the original Edwards-Anderson model<sup>5</sup> there is no longer a transition in finite field because the order parameter  $q$  is then always nonzero. However, de Almeida and Thouless<sup>6</sup> showed that the Sherrington-Kirkpatrick<sup>7</sup> (SK) model for classical Ising spins exhibited an instability for purely random interactions in the presence of a field. This instability has been interpreted

as a phase transition line by Toulouse,<sup>8</sup> denoted by  $T_G(H)$ . Toulouse and Gabay<sup>9(a)</sup> and Gabay and Toulouse<sup>9(b)</sup> have extended this calculation to the SK model for classical  $m$ -component spins. Van-nimicus *et al.*<sup>10</sup> have studied the entire  $H-T$  phase diagram for the PaT (Parisi-Toulouse) hypothesis. They argue that, at fixed field, on reducing the temperature the system first undergoes a crossover [at  $T_X(H)$ ] from paramagnetic (Curie-like) behavior to a region where the susceptibility is nonlinear. Only at the lower temperature,  $T_G(H) < T_G(0)$ , does the system enter the spin-glass phase.

This paper is mainly concerned with the experimental definitions of the spin-glass transition temperature,  $T_G(H)$ , and of the crossover temperature,  $T_X(H)$ , and with the measurement of their field dependences. We have studied the Ag:Mn spin-glass using low-field, high-resolution dc magnetization measurements. Very recently Monod and Bouchiat have used criteria different from our own for the same purpose.<sup>11</sup>

Section II describes the sample preparation techniques, the SQUID magnetometer, and the measurement procedure. Section III reviews some of the pertinent experimental facts. Section IV outlines our experimental results and describes the technique for determining a number of characteristic temperatures

from the structure exhibited by  $dM(H,T)/dT$ . Section V discusses the significance of the various temperatures in both phenomenological and theoretical terms and then compares their field dependences with those predicted by current theories. We finally compare the nonlinearity of the experimental susceptibility with the theoretical predictions below, at, and above  $T_G$ .

## II. EXPERIMENTAL

### A. Sample preparation

Two samples containing 2.6 and 4.0 at. % Mn were each prepared by arc melting the appropriate quantities of 99.999% pure Ag and 99.99% pure Mn under 1 atm of 99.999% pure argon.<sup>12</sup> The buttons were then inverted and remelted ten times at full arc power. The resulting ingots, circa 2.5 g, were next annealed at 835°C under 1 atm of argon for 13 h and then cooled rapidly to room temperature. The ingots were etched lightly in dilute HNO<sub>3</sub> and then rolled to a thickness of  $\sim 220 \mu\text{m}$ . The foil samples were then given a second anneal identical to the first. The measurement samples used, circa 60 mg, were cut from the center of the foils. We have found previously<sup>13</sup> that the above procedure gives samples with a homogeneous concentration of magnetic impurity throughout the sample. The particular samples used here were checked for gross inhomogeneities by measuring the low-field glass temperature of samples taken from various parts of the (100 mm long) foil. The resulting  $\Delta T_G/T_G$  was always less than 0.4%.

### B. SQUID magnetometer

The magnetizations were measured using a simple SQUID magnetometer. Two counterwound superconducting pick-up coils are mounted on the outside of a vertical quartz tube. This tube fits inside a superconducting solenoid. The solenoid, tube, and the commercial SQUID probe<sup>14</sup> to which the pick-up coils are attached are mounted rigidly together and are immersed in a helium bath. A second quartz tube fits inside the first. The second tube contains a vertical coil-foil copper wire shield; at the top of this is a heater, at the bottom a carbon-glass resistor. The sample hangs inside the foil shield in a Teflon bucket. The space between the two tubes and the sample space can be evacuated or filled with helium gas. The sample temperature can be raised from 4.2 to  $\sim 150$  K without difficulty. The measurement field can be varied from 0.5 to 500 Oe. On occasions, a mumetal shield has been added to reduce the minimum usable measurement field to 40 mOe.

A determination of the absolute magnetization is made by moving the sample from one pick-up coil to

the other. A sample of manganese Tutton salt  $\text{Mn}(\text{NH}_4)_2(\text{SO}_4)_2 \cdot 6\text{H}_2\text{O}$  is used as calibrant. The stability and the small temperature-dependent background of this magnetometer allow us to measure the temperature dependence of the sample magnetization by slowly sweeping the temperature and observing the SQUID output. In this mode, the  $M(T)$  data are recorded on magnetic tape by a computer based system.

### C. Measurement procedure

Figure 1 illustrates the two measurement procedures used to obtain the two different behaviors of  $M(T)$ . The sample is first cooled in near-zero field (typically 0.5 Oe) to below  $T_M(1 \rightarrow 2)$ .  $T_M$  is the temperature at which the maximum in the magnetization is expected to occur. Next the measurement field is applied, causing an instantaneous ( $t < 10$  s) rise in the magnetization ( $2 \rightarrow 3$ ). The temperature is then increased and the zero-field-cooled (ZFC) warming curve ( $3 \rightarrow 4 \rightarrow 5$ ) is recorded. The temperature is next reduced without changing the measurement field ( $5 \rightarrow 4 \rightarrow 6$ ), then increased again and the field-cooled (FC) warming curve ( $6 \rightarrow 4 \rightarrow 5$ ) is recorded. Both warming sweeps are made at the same rate (typically  $50 \text{ mKs}^{-1}$ ) to minimize the effect of any thermal lag between the sensor and the sample. The magnetization was measured at temperature intervals of 0.1–1 K in the range  $T_m/2$  to  $2T_m$ , except in the neighborhood of  $T_M$  where data points were taken at 30- to 50-mK intervals. This procedure was repeated at several measuring fields in the range  $0.5 \leq H \leq 500$  Oe.

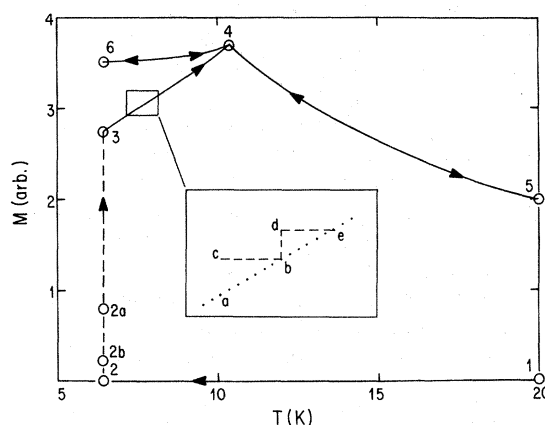


FIG. 1. Typical magnetization vs temperature measuring cycle for the Ag:Mn 2.6 at. % sample in 6 Oe.  $1 \rightarrow 2 \rightarrow 3 \rightarrow 4 \rightarrow 5$  is designated the zero-field-cooled (ZFC) cycle and  $5 \rightarrow 4 \rightarrow 6 \rightarrow 4 \rightarrow 5$  the field-cooled (FC) cycle. The data are taken on warming at the same rate in both cases.  $T_M$  denotes the temperature at which the maximum in magnetization occurs for a given field. The insert to this figure is schematic.

### III. BRIEF EXPERIMENTAL REVIEW

It will be useful to summarize here some of the better known spin-glass idiosyncrasies<sup>2,3</sup> seen in dc magnetization measurements. This can be done conveniently with reference to Fig. 1. In, say, the  $t \rightarrow 0.1$  s limit, the value of  $(M/H)$  corresponding to the magnetization (2  $\rightarrow$  3) is equal to the ac susceptibility which would be measured at 10 Hz. If the warming (at rate  $dT/dt = +k$ ) (3  $\rightarrow$  4) is stopped (point  $b$  on the insert to Fig. 1) and the temperature is then lowered (at rate  $-k$ ) the magnetization remains roughly constant ( $b \rightarrow c$ ). On rewarming (at rate  $+k$ ),  $M(T)$  follows ( $c \rightarrow b$ ), *not* a curve through  $c$  parallel to ( $a \rightarrow b \rightarrow e$ ). If the temperature is held constant at some point  $b$ , then the magnetization increases with time ( $b \rightarrow d$ ) in a quasilogarithmic manner,

$$M(t) \approx M_b + A(T_b) \ln t \quad (1)$$

This is often termed the growth of the isothermal remanent magnetization,  $\sigma_{IRM}$ .<sup>15</sup> On further warming from  $d$  (at rate  $+k$ ), the magnetization is again constant ( $d \rightarrow e$ ) until the original ZFC curve is reached. Qualitatively, the ZFC magnetization resembles the ac susceptibility. However, at each temperature there is a slow time evolution of the form given by Eq. (1), and, since the entire sweep (3  $\rightarrow$  4) takes finite time (typically several minutes), any value of  $\chi$  derived from such a ZFC measurement is always greater than that obtained from an ac measurement of modest ( $\approx 10$  Hz) frequencies. In contrast, the FC response below  $T_M$  appears to be strictly time independent. Our measurements indicate  $dM(H, T)/dt < xM(H, T)$  where  $x \approx 10^{-5} \text{ s}^{-1}$ . Recent measurements with a very high stability apparatus<sup>16</sup> find  $x \approx 6 \times 10^{-8} \text{ s}^{-1}$ . Thus, experimentally, the FC magnetization (6  $\rightarrow$  4) appears to correspond to dynamic, and possibly thermodynamic, equilibrium in the spin-glass state. Knitter and Kouvel<sup>17</sup> have used a different field cycling experiment to come to the same conclusion. The calculations of Toulouse<sup>8</sup> and of Vannimenus *et al.*<sup>10</sup> rest on the hypothesis<sup>18</sup> that the FC state is indeed a state of thermodynamic equilibrium. This is, however, in direct conflict with the latest Monte Carlo calculations of Morgenstern and Binder,<sup>19</sup> which suggest that any apparent transition is an artifact of finite measuring time.

The thermoremanent magnetization,  $\sigma_{TRM}$ , is defined<sup>15</sup> as the remanent magnetization the sample possesses when, after cooling below  $T_M$  in an applied field, this field is reduced to zero (e.g., 5  $\rightarrow$  4  $\rightarrow$  3  $\rightarrow$  2a). This thermoremanent magnetization then decays quasilogarithmically in time. The isothermal remanent magnetization,  $\sigma_{IRM}$ , is the (zero-field) remanence measured after ZFC and application of the field for only a finite time (e.g., 1  $\rightarrow$  2  $\rightarrow$  3  $\rightarrow$  2b);

$\sigma_{IRM}$  also decays quasilogarithmically in time.

The low-temperature spin-glass magnetization is often described<sup>15</sup> as consisting of two parts: a reversible component  $M_{rev}$ , which is time independent, i.e., a function only of temperature and field, and an irreversible (remanent) component,  $M_{irr}$ , which depends both on time and on the thermomagnetic history of the sample. In very low fields and short measurement times, where  $\sigma_{IRM}$  is vanishingly small, any irreversible component in  $M_{ZFC}$  may be ignored such that  $M_{ZFC} \approx M_{rev}(H, T)$ . However, in higher fields  $\sigma_{IRM}$  is not negligible and a significant portion of  $M_{ZFC}$  is irreversible. The ZFC magnetization below  $T_M$  is then written

$$M_{ZFC}(H, T, t) = M_{rev}(H, T) + M_{irr}(H, T, t) \quad (2)$$

where  $M_{irr}$  (which would be equal to the  $\sigma_{IRM}$  measured immediately after suppression of the field) is the quasilogarithmic term from Eq. (1) and  $M_{rev}/H$  is the  $t \rightarrow 0$  limit, or the ac susceptibility. This decomposition is somewhat misleading. First, since  $\chi_{ac}$  depends on frequency for  $T < T_M$ ,<sup>20</sup> the separation of  $M_{rev}$  and  $M_{irr}$  depends on the time scale chosen. Furthermore, the  $t \rightarrow 0$  limit has yet to be determined. Second, Eq. (2) suggests an independence of the temperature variations of  $M_{rev}$  and  $M_{irr}$  which is not observed; in particular reference to Fig. 1, on warming  $d \rightarrow e$ , the magnetization does *not* have the same temperature dependence as the ac susceptibility, as Eq. (2) would imply.

### IV. EXPERIMENTAL RESULTS

A representative set of magnetization curves in various applied fields is shown in Fig. 2. The apparent smearing of the transition by the field is clear; compare 500 (Fig. 2) with 6 Oe (Fig. 1). The transition region can be very loosely defined as being between the "reversibility" temperature  $T_R(H)$ <sup>13</sup> (above which the ZFC and FC magnetizations are indistinguishable), and the "break" temperature  $T_B(H)$ <sup>21</sup> (below which the magnetization "breaks away" from a Curie-like behavior). As an example, we have fitted (dash-dotted line Fig. 2) a Curie behavior to the 340-Oe experimental points above 15 K. Below  $T_B$ , the finite field susceptibility ( $M/H$ ) is nonlinear in  $H$ . The approximate behavior of  $T_R$ ,  $T_B$ , and  $T_M$  are indicated by the dashed lines in Fig. 2. For vanishingly small fields these three temperatures coalesce into a single well-defined glass temperature,  $T_G^0(H \rightarrow 0)$ . Experimentally,  $T_G^0$  was determined from measurements of  $T_M$  made in fields  $\sim 1$  Oe.

To analyze in detail the behavior in the transition region, we have examined the temperature derivative of the magnetization,  $dM(H, T)/dT$ , as a function of temperature for both FC and ZFC cases. This was

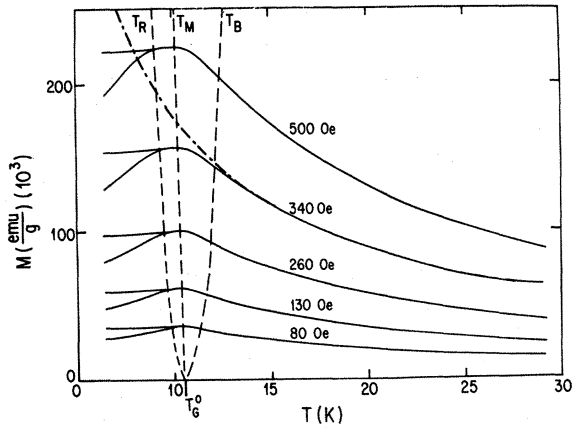


FIG. 2. Typical magnetization vs temperature data in various measuring fields for the Ag:Mn 2.6 at. % sample. The dot-dashed line through the 340-Oe data points is a Curie behavior fitted to the points above 15 K. The dashed lines indicate the approximate field dependences of  $T_R$ ,  $T_B$ , and  $T_M$ .

done by taking the point by point differences in the digital  $M(T)$  data. Figure 3 shows typical examples of high- and low-field behavior. For convenience, we have plotted here  $(M/H)$  rather than  $M$ . This also serves to illustrate the nonlinearity of the susceptibility below  $T_B$ . The derivative curve,  $a'$ , of the low-

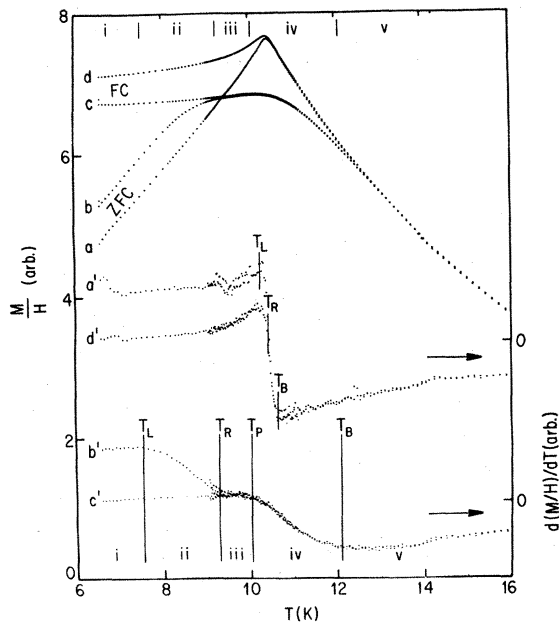


FIG. 3.  $M/H$  vs  $T$  (upper) and  $dM(H,T)/dT$  vs  $T$  (lower) data for the 2.6 at. % Ag:Mn sample in 6 ( $a$ ,  $a'$ , and  $d$ ) and 430 Oe ( $b$ ,  $b'$ , and  $c'$ ). The significance of regions (i)–(iv) is explained in the text.

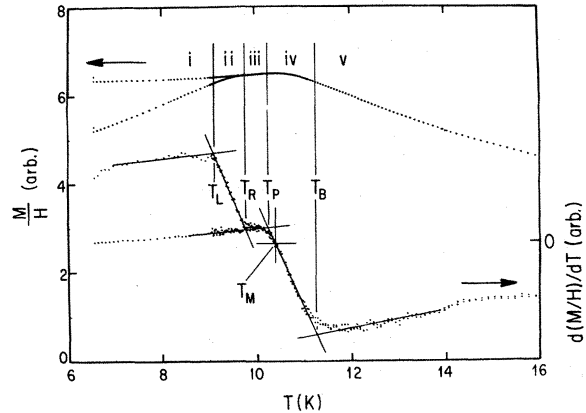


FIG. 4.  $M/H$  vs  $T$  (upper) and  $dM(H,T)/dT$  vs  $T$  data for the 2.6 at. % Ag:Mn sample in 130 Oe. The straight lines through the data points determine the characteristic temperatures  $T_L$ ,  $T_R$ ,  $T_P$ , and  $T_B$  as discussed in Sec. IV.

field ZFC curve,  $a$ , shows the expected sharp change in sign around  $T_M$  (given by  $dM/dT=0$ ). From our definition above,  $T_R$  is the temperature at which the derivative curve,  $d'$ , of the low-field FC curve,  $d$ , meets curve  $a'$ . We note that  $T_R \approx T_M$  at low fields.<sup>13</sup> For this field (6 Oe) the maximum and minimum values of  $a'$  occur at slightly different temperatures ( $\Delta T \approx 0.24$  K). We will show below that the former corresponds to  $T_L$  (to be defined) and the latter to  $T_B$ . In lower fields the difference  $T_B - T_L$  decreases still further ( $\approx 0.18$  K for the 2.6 at. % sample in 0.5 Oe).

The derivative,  $b'$ , of the ZFC curve measured at higher field (430 Oe) can be divided into five rather distinct temperature regions.  $dM/dT$  appears (i) to be fairly constant up to  $T_L$ , (ii) to decrease sharply between  $T_L$  and  $T_F$ , (iii) to decrease more slowly between  $T_R$  and  $T_P$ , (iv) to decrease sharply to  $T_B$ , and (v) to behave as  $-1/T^2$  above  $T_B$ . The various characteristic temperatures were obtained from the intersections of the straight lines drawn through  $dM/dT$  in the temperature regions delineated above. Figure 4 shows this procedure rather clearly for a measuring field of 130 Oe.  $T_L$  is thus the temperature where the ZFC warming curve begins to deviate from its apparently linear slope.  $T_P$  is the end point of the region in which  $M \neq T$  (beginning at  $T_R$ ) and hence marks the end of a "plateau" region in  $dM/dT$ .

## V. DISCUSSION

We now discuss the significance of the five regions and four temperatures we have just defined, first in phenomenological terms, and then in terms of current theories. We then compare our experimental

results with the theoretical relations predicted by Gaby and Toulouse<sup>9</sup> and by Vannimenus *et al.*<sup>10</sup>

### A. Phenomenological

In region (i) of Fig. 3, the deduced FC and ZFC susceptibilities both show nonlinearity with  $H$ . The ZFC susceptibility increases more rapidly than  $H$ ,

$$[M_{\text{ZFC}}(H_1)/H_1 > M_{\text{ZFC}}(H_0)/H_0] \text{ with } H_1 > H_0,$$

while the FC susceptibility increases more slowly than  $H$ ,

$$M_{\text{ZFC}}(H_1)/H_1 < M_{\text{FC}}(H_0)/H_0.$$

These two observations are consistent with the respective nonlinear field dependences of  $\sigma_{\text{IRM}}$  and  $\sigma_{\text{TRM}}$  at fixed temperature. Thus in the spirit of Eq. (2), the ZFC magnetization is  $(M_{\text{rev}} + \sigma_{\text{IRM}})$ ; while the FC magnetization is  $(M_{\text{rev}} + \sigma_{\text{TRM}})$ . The fact that in region (i) the high- and low-field ZFC curves appear to be parallel is puzzling. At first sight this would seem to confirm the correctness of Eq. (2):  $\sigma_{\text{IRM}}$  has been increased by the larger field, but the dominant temperature dependence is still contained in  $M_{\text{rev}}$ . Two errors in this interpretation have already been discussed at the end of Sec. III. However, if one uses the strict definition of  $\sigma_{\text{IRM}}$  (the remanent magnetization after the measuring field has been suppressed), then the parallelism of the high- and low-field ZFC curves implies that the temperature dependence of  $\sigma_{\text{IRM}}$  is ignorable in region (i) for the field and temperature range of our measurements. We note that the maximum in  $\sigma_{\text{IRM}}$  occurs at a temperature near to  $T_L$ ,<sup>22</sup> and suggest that  $T_L(H)$  is the temperature above which  $\sigma_{\text{IRM}}$  has a significant temperature dependence.

As the temperature is further increased through region (ii), the ZFC and FC curves eventually meet at  $T_R(H)$ . This occurs when the saturated remanence corresponding to  $T_R$ ,  $\sigma_{\text{sat}}(T_R)$ , which is decreasing with increasing temperature, becomes equal to  $\sigma_{\text{IRM}}$  of the sample. Above  $T_R(H)$  the magnetization is time independent and reversible with temperature. It should be noted that the value obtained here for  $T_R(H)$  depends on  $dT/dt$ . If the sweep rate is decreased significantly (factor of 10) from the value used to generate Fig. 1,  $dT/dt = 50$  mK/s,  $T_R(H)$  occurs at lower temperatures. Increasing the sweep rate by a factor of 10 above this value of  $dT/dt$  leads to serious discrepancies between the temperature of the sample and that of the thermometer. We are therefore unable to say with any certainty if  $T_R(H)$  increases when using more rapid temperature sweeps. We strongly suspect, however, that it does. One may also regard  $T_R(H_1)$  as the temperature at which, after application of a dc field  $H_1$ ,

the magnetization appears “reversible” (attains a time independent value) *within the time scale* of our particular experiment.

We can imagine making an ac susceptibility measurement at an extremely low frequency with an oscillating field magnitude  $H_1$ . One would then expect  $\chi_{\text{ac}}(\nu, H_1)$  to have (approximately) the same form as the ZFC curve measured in  $H_1$ . This suggests therefore that very low frequency  $\chi_{\text{ac}}$  will be highly nonlinear in  $H_{\text{osc}}$  in regions (i), (ii), and (iii). Further, this nonlinearity will be dramatically reduced as the frequency is increased. At frequencies  $>1$  Hz, no nonlinear behavior of  $\chi_{\text{ac}}$  has been observed<sup>20</sup> for  $0.1 \leq H_{\text{osc}} \leq 10$  Oe.

It is next relevant to ask at what temperature the ac response, measured at moderate frequency and small oscillating field (say 10 Hz and 1 Oe), in the presence of an external static field,  $H_1$ , would meet the  $(M/H_1)$  FC and ZFC curves. The rounding of the ac response by an external static field is fairly symmetric about  $T_M$ .<sup>20</sup> However, while the FC and ZFC curves have much the same rounding above  $T_M$  as the ac response, below  $T_M$  they exhibit the “plateau” not seen in the ac measurements. While we do not have ac susceptibility data for this particular field range, we suggest that  $T_P$  can be taken as the temperature below which the ac ( $t$  small) and dc ( $t \rightarrow \infty$ ) responses in the presence of a field will be different. More specifically,  $T_P(H)$  is the temperature below which  $\chi_{\text{dc}} = M/H_{\text{static}} > \chi_{\text{ac}}(\nu, H_{\text{osc}}, H_{\text{static}})$  where  $H_{\text{static}}$  is the dc field,  $H_{\text{osc}}$  the ac field, and  $\nu$  the frequency. In Sec. VB we shall argue that  $T_P(H)$  is to be identified with  $T_G(H)$ . We should perhaps note that  $T_P$  and  $T_M$  are virtually coincident in our field range, and any distinction between them may be irrelevant.

### B. Comparison with theory for $T_G(H)$ and $T_X(H)$

The SK model<sup>7</sup> assumes an infinite range interaction whose strength is distributed with variance  $J$  about an average interaction  $J_0$ . The high temperature Curie-Weiss  $\Theta$  can be taken as a measure of  $J_0$ .<sup>23</sup> In the noble metal-Mn spin-glasses,  $\Theta$  changes sign at characteristic concentration,  $\sim 2.5$  at. % for Ag:Mn.<sup>24</sup> For our 2.6 at. % sample, we are therefore confident that  $H_0/J = \kappa\Theta/T_G \approx 0$ . However, for the 4 at. % sample,  $\Theta \approx 10$  K and  $T_G = 15$  K giving  $\Theta/T_G \approx 0.7$ . The Au:Fe system, at 14 at. % Fe, exhibits<sup>25</sup> the paramagnetic to ferromagnetic to spin-glass behavior predicted by the SK model for  $J_0/J \geq 1$ . For Au:Fe 14 at. % Fe,  $\Theta \approx 130$  K,<sup>26</sup> and  $T_G \approx 40$  K.<sup>27</sup> Hence  $\Theta/T_G \approx 3$  for  $J_0/J = 1$  and  $\kappa \approx 3$ . On the most naive level this implies that for our Ag:Mn 4 at. % sample  $J_0/J \leq 0.22$ . Given this relatively small value, and the fact that  $T_G(H)$  has only been calculated for  $J_0 = 0$ , we have proceeded to

compare our results on both the 2.6 and 4 at. % samples with the theory.

The predicted<sup>6,9</sup> mean-field value of  $T_G(H)$  for  $J_0=0$ , written in terms of the dimensionless variable  $h = H/J = g\mu_B H/k_B T_G^0$ , is given by<sup>9</sup>

$$h^{2/3} = [4/(m+2)]^{1/3} \{1 - [T_G(H)/T_G^0]\}, \quad (3)$$

where  $m$  is the spin dimensionality ( $m=1$  for the Ising case and  $m=3$  for the Heisenberg case). We show in Fig. 5 the various reduced temperatures ( $T_L/T_G^0$ , etc.) as functions of the reduced field  $h = g\mu_B H/k_B T_G^0$  for the two samples measured. The solid curves in Fig. 5 are the theoretical predictions with no adjustable parameters for  $m=1$  and 3. Figure 6 is an expanded version of Fig. 5 showing only  $T_P/T_G^0$ ; the data for the two samples appear to scale with  $T_G^0$  (i.e.,  $J$  in mean field). The agreement between our measurements and the theoretical predictions, which are relatively insensitive to the choice of  $m$  in (3), strongly suggest the identification of  $T_P$  as the experimental manifestation of  $T_G(H)$ . How-

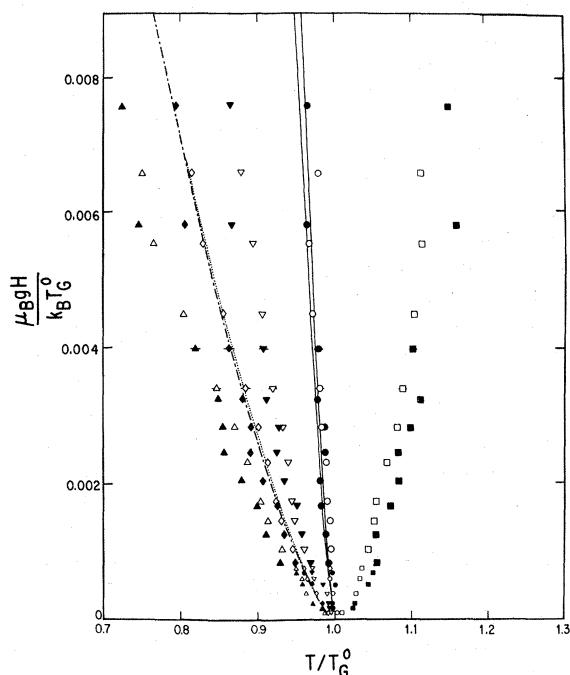


FIG. 5. The dependence on reduced field  $g\mu_B H/k_B T_G^0$  of the reduced temperatures  $T_L/T_G^0$ ,  $\Delta$ ,  $\blacktriangle$ ;  $\bar{T}/T_G^0$ ,  $\diamond$ ,  $\blacklozenge$ ;  $T_R/T_G^0$ ,  $\nabla$ ,  $\blacktriangledown$ ;  $T_P/T_G^0$ ,  $\circ$ ,  $\bullet$ ; and  $T_B/T_G^0$ ,  $\square$ ,  $\blacksquare$ . Open symbols, 2.6 at. % Mn; closed symbols, 4.0 at. % Mn. The dot-dashed and dotted lines are the best fits (see text) to  $\bar{T}$  for the 2.6 and 4.0% samples, respectively. The solid lines are the theoretical predictions for  $T_G(H)$  for  $m=1$  and 3.

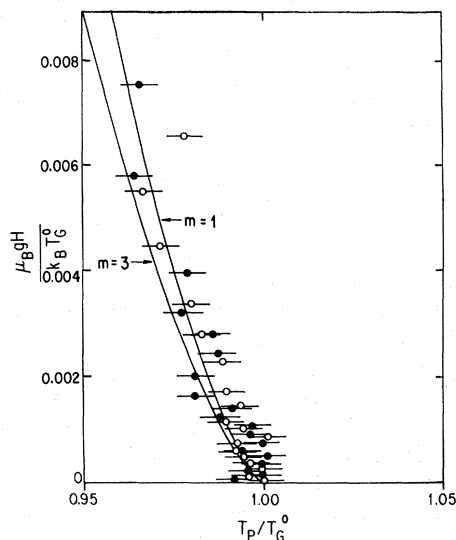


FIG. 6. The dependence on reduced field  $g\mu_B H/k_B T$  of  $T_P/T_G^0$ .  $\circ$ , 2.6 at. % Ag:Mn;  $\bullet$ , 4.0 at. % Ag:Mn. The solid lines are the theoretical predictions for  $m=1$  and 3.

ever, measurements to higher fields (or on less concentrated samples) are needed before the correctness of the theory and the choice of  $T_P$  as  $T_G(H)$  is established.

As seen in Fig. 5, the experimental values for  $T_B(H)$  do not scale particularly well with  $T_G^0$ . This is perhaps not too surprising.  $T_B(H)$  is the center of a crossover region rather than the well-defined temperature that we have attempted to extract from our data. The best power law fits of the form  $(1 - T_B/T_G^0) = b(h)^\beta$  give  $\beta = 0.51 \pm 0.1$  and  $0.56 \pm 0.1$ ; and  $b = 1.6 \pm 1.0$  and  $2.3 \pm 1.0$  for the 2.6 and 4.0 at. % samples, respectively. These exponents are in reasonable agreement with the value of 0.5 found previously from ac measurements in a transverse dc field.<sup>28</sup>

It is intriguing to note that, although  $T_L(H)$  and  $T_R(H)$  do not scale well with  $T_G^0$ , the mean of these two temperatures does, viz.,  $\bar{T} = [T_L(H) + T_R(H)]/2$ . This temperature effectively defines the center of the transition region (ii) between the spin-glass (i) and "reversible" (iii) behaviors. Further, the best fit of the data to a power law of the form  $[1 - \bar{T}(H)/T_G^0] = a(h)^\alpha$  gives  $\alpha = 0.71 \pm 0.05$ ,  $a = 6.7 \pm 1.0$  (dot-dashed line Fig. 5), and  $\alpha = 0.69 \pm 0.05$ ,  $a = 6.1 \pm 1.0$  (dotted line Fig. 5) for the 2.6 and 4.0% samples, respectively. The experimental values of  $\alpha$  are thus very close to the theoretical exponent of  $\frac{2}{3}$ . The disagreement with theory is in the value of the prefactor in Eq. (3). The magni-

tude of the field variation of  $\bar{T}(H)$  is too large; to obtain agreement ( $h_{\text{theor}}/h_{\text{expt}} \approx 19$ ).

There is a certain beguiling symmetry about the  $H$ - $T$  diagram containing  $\bar{T}(H)$  and  $T_B(H)$ .  $\bar{T}(H)$  is the mean temperature above which there is no longer any viscous response of the magnetization on the particular time scale of our experiment. The experimental value of  $\alpha$  is close to  $\frac{2}{3}$ . One may thus legitimately ask the value of  $\alpha$  which would be obtained if the experimental time scale were reduced. We expect the limit ( $t$  very small) value of  $\bar{T}(H)$  to be  $T_P(H)$ ; this we claim can also be fitted with the same exponent. We therefore tentatively suggest that  $[1 - \bar{T}(H)]$  will always behave as  $h^{2/3}$  independent of the time scale of the experiment, at least over the field ranges used in our experiments.

No specific calculation exists for  $T_X(H)$ .<sup>29</sup> The appearance of a nonlinear field term in  $M/H$  at temperatures  $T > T_G(H)$  has been predicted by Toulouse and Gabay<sup>9(a)</sup> for the  $m$ -component Heisenberg spins in the infinite range SK model. It is tempting to adapt that result to our measurements. In particular, we have attempted to identify  $T_B(H)$  with the crossover temperature  $T_X(H)$ . We have tried to extract the form of  $T_X(H)$  from the expression of Vannimenus *et al.*<sup>10</sup> for  $M/H(T)$  above  $T_G(H)$ . We simply took  $T_X(H)$  as the temperature where  $M/H(T)$  had deviated from a  $1/T$  behavior by some small arbitrary amount, say 0.5%. Unfortunately, the curvature of  $T_X(H)$  so obtained is opposite to that of  $T_B(H)$  in the low-field range of our measurements. However, the temperature dependence at *fixed field* above  $T_G(H)$  does fit rather well with their expression until one is close to  $T_G(H)$ , where the expansion breaks down. This is discussed further in Sec. V C. For the moment, we suggest an identification of  $T_B(H)$  with  $T_X(H)$ , though we are left without theoretical justification.

It has been conjectured<sup>4,5</sup> that below  $T_G$  the configurational energy of the spin-glass becomes a labyrinthine surface in configurational space. This surface possesses many quasidegenerate ground-state minima (QDM's), lying within a narrow bandwidth. There will always be one QDM which is the true (i.e., lowest) ground state of the system. However, the mutual inaccessibility of the QDM's and the small energy differences between them lead to the system becoming stabilized in one of the QDM's on cooling through the glass temperature. This approach naturally yields the broken ergodicity which is thought to be necessary to explain, in particular, the behavior of the specific heat<sup>30</sup> in spin-glasses. The essential correctness of this picture is confirmed by the computer simulations of Walker and Walstedt<sup>31</sup> of the Ruderman-Kittel (-Kasuya)-Yosida spin-glass and more recently by those of Bantilan and Palmer<sup>32</sup> for the Ising SK model. Both simulations have been made at  $T=0$ . However, it is to be expected that the

energy surface in configurational space characteristic of the spin-glass phase develops very rapidly in a small temperature interval around  $T_G$  and then remains essentially temperature independent below  $T_G$ .

Bantilan and Palmer<sup>32</sup> have studied particularly the effect of a magnetic field on the configurational energy. In their simulations on 100 spins, they find the true ground state of this system (sample) for a given set of exchange couplings  $\{J_{ij}\}$ . This procedure is then repeated for  $\sim 50$  different sets (samples) of  $\{J_{ij}\}$ 's. The resulting set of "true ground states" may then be viewed as the QDM's referred to above. After field cooling, Bantilan and Palmer find a given sample to be in its true ground state, in which it stays. This is in agreement with the Parisi-Toulouse hypothesis<sup>18</sup> that the FC state corresponds to a thermodynamic equilibrium state. After ZFC, the sample is also found to be in its true ground state. However, the subsequent application of a magnetic field moves the position of the true ground state some distance in configuration space, far from the (relatively unchanged) sample configuration. The sample rapidly finds the nearest local minimum and then, over a rather long time, finds its way into the true ground state. Any point on the ZFC magnetization curves thus corresponds to the system being in a metastable local minimum. In this picture the FC magnetization curves correspond to the system in one QDM. After ZFC the system is also in one QDM. Application of the field essentially "scrambles" the configuration surface and the system rapidly finds the nearest local minimum whose energy is somewhat above the band containing the QDM's. The quasilogarithmic time dependence, or magnetic viscosity, then comes from the movement in configuration space from the local minimum to the nearest QDM.

The change of the energy surface in configuration space with field seemingly must take place continuously. Hence, if below  $T_G$  one changes the experimental dc field by a small enough amount, one should see a reversible change in the magnetization. We have searched for such reversible behavior at  $T_G/2$  in fields as low as 40 mOe (having cooled in fields of  $< 1$  Oe) and have always found quasilogarithmic time dependences. Other attempts to observe reversible behavior below a threshold field have also been unsuccessful.<sup>33</sup> Thus, even for very small fields, it seems that the changes in the energy surface are extremely dramatic—any change in the field truly "scrambles" the surface.

In the spirit of this model, we expect the energy surface to be relatively featureless above  $T_G^0$  or  $T_X(H)$ . In this region we also expect the ac and dc susceptibilities to be strictly identical since  $M \propto H$ .

Between  $T_X(H)$  and  $T_G(H)$  we expect the energy surface to contain many local minima between which the system can move relatively easily. One might in-

tuitively expect there to be some frequency dependence to this movement. However, in this transition region, to the extent that  $M$  is linear in  $H$ , the low ( $\sim 1$  Hz) frequency ac susceptibility,  $\chi_{ac}(\nu, H_{osc}, H_{static}) \approx \chi_{dc}(H_{static})$ .

$T_G^0$  or  $T_G(H)$  are the temperatures at which the QDM's appear, i.e., some minima in the energy surface suddenly become sufficiently deep that they are mutually inaccessible. For  $T < T_G(H)$ , the experimentally observed  $M_{FC} > M_{ZFC}$  implies  $M(\text{QDM}) > M(\text{local min.})$ . One could extend this idea further to expect that  $M(\text{local min. } b) > M(\text{local min. } a)$  if  $E_b < E_a$ .

Well below  $T_G(H)$  the difference between the FC dc response and the ac response in the presence of an external field depends dramatically on frequency from dc to (say) 1 Hz. Measuring  $\chi_{ac}$  at  $T < T_G(H)$  (after FC in any static field  $H_1$ ) with a small oscillating field ( $\sim 1$  Oe) and at moderate frequencies ( $\sim 1$  Hz) never allows the system to move far in configuration space from the QDM achieved after FC. The resultant  $\chi_{ac}$ , which decreases with decreasing temperature, is as expected from linear response theory<sup>32</sup>; the system is sampling the bottom of the QDM. In fact, the ac response at  $\geq 1$  Hz appears independent of whether the system is in a local minimum or a QDM:  $\chi_{ac}$  in an external static field after ZFC is experimentally indistinguishable from the FC result.<sup>20</sup> Presumably the curvature of the bottom of the local minimum is much like that of the QDM.

The finite field FC  $\chi_{dc}$  (the  $t \rightarrow \infty$  limit), however, apparently does violate linear response theory.  $M/H_1$  is temperature independent, unlike the  $\chi(T) \propto T$  for  $T < T_G$  derived using linear response.<sup>32</sup> Bantilan and Palmer suggest that this results from the broken ergodicity—the system is locked in one QDM. We therefore suggest that the system enters the spin-glass phase at  $T_G(H)$ , where the predictions of linear response theory break down: when  $\chi_{dc} = M/H_{static} > \chi_{ac}(\nu, H_{osc}, H_{static})$ . We have argued in Sec. V A that this occurs experimentally at  $T_P(H)$ . Hence we identify  $T_P(H)$  as  $T_G(H)$ .

$T_R(H)$ , which we have defined as the temperature at which the FC and ZFC curves meet, is also the temperature above which the system, after ZFC, finds its way immediately (on the time scale of a particular experiment) into a QDM. It is thus not necessarily the temperature at which the QDM's disappear with increasing temperature. However,  $T_R(H)$  does give information about how far the system can move in configuration space for a particular  $(T, H)$  within an implicit experimental time.

The behavior shown in the insert of Fig. 1 of the ZFC magnetization with temperature can now be interpreted in terms of this model. At (a) the system is in a local minimum of depth  $\Delta \approx T_a$  from which it is slowly moving towards a QDM. Raising the tem-

perature to  $T_b$  allows the system to move across any barriers of height  $\Delta < T_b$  to find a lower local minimum at (b), hence increasing the magnetization. Decreasing the temperature from (b) to (c) simply maintains the system in the same local minimum. Holding the temperature constant for a relatively long period at (b) again allows the quasilogarithmic evolution of the magnetization. After some time the system has achieved a magnetization (d). We suggest that this corresponds to the system having moved into a minimum of depth  $\Delta \approx T_e$ , since a relatively rapid increase of the temperature to (e) (so that effectively no motion in configuration space takes place) does *not* result in any further increase in magnetization (decrease in system energy) until the system has thermal energy  $T_e$ .

### C. Comparison with theory for $M(H, T)$

Toulouse and Gabay<sup>9(a)</sup> have derived expressions for  $M(H, T)$  for  $m$ -component Heisenberg spins in the infinite range SK model. For  $T > T_G^0$  they find in reduced units ( $m = 3$ ):

$$M/H = (1/T) \{ 1 - H^2 \frac{1}{5} [(T^2 + 4)/(T^2 - 1) - 6/(5T^2 - 3)] + O(H^4) \}, \quad (4)$$

while for  $T = T_G^0$  ( $m = 3$ ),

$$M/H = 1 - (1/\sqrt{2})H + \frac{35}{40}H^2 + O(H^3). \quad (5)$$

For  $T < T_G^0$ , they introduce the PaT hypothesis, and obtain

$$M/H = 1 - \frac{3}{4} [4/(m+2)]^{1/3} H^{4/3}. \quad (6)$$

We have used as the reduced field [see Eq. (3)],  $H/J = g\mu_B H/k_B T_G^0$ . We find the experimental field variation to be much greater than that predicted by Eqs. (4)–(6). For example, for  $T > T_G^0$ , we fix  $H/J$  and fit to the temperature dependence of  $M/H$ . Our results (dotted points) and Eq. (4) (solid line) are plotted in Fig. 7. The field  $H/J$  has been taken as a fixed parameter, obtained from a least-squares fit. We find that  $H/J$  must be increased by a factor of 28 and 18 for fields of 220 and 500 Oe, respectively. Therefore this field scale factor is a function of field. This is troublesome, since the mean-field theory should be most precise in this region, but might be an artifact of the asymptotic nature of Eq. (4).

The situation appears to be more satisfactory for  $T = T_G^0$  (Fig. 8, line a) and  $T < T_G^0$  (Fig. 8, line b). The open and closed circles are the experimental points, the solid lines Eqs. (5) and (6), respectively. Both curves require a correction factor to the field scale rather close to one another. At  $T = T_G^0$ , the



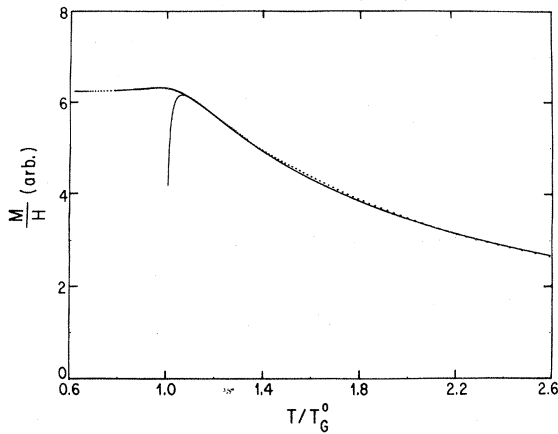


FIG. 7. The temperature dependence of  $M/H$  for the 2.6 at. % Ag:Mn sample in a magnetic field of 500 Oe. The solid line is the best fit of the data to Eq. (4) (see text), and results in  $H/J = 0.12 \approx 18(g\mu_B H/k_B T_G^0)$ .

least-squares fit requires that  $H/J$  be multiplied by a factor of 18;  $T < T_G^0$ , the multiplication factor is 15. The latter multiplication factor is independent of temperature in the low-temperature regime where the field-cooled magnetization curve is experimentally temperature independent ( $T < 8$  K for the 2.6 at. % Ag:Mn sample with  $T_G^0 = 10.45$  K), in agreement with the PaT hypothesis. At temperatures where the field-cooled magnetization varies with temperature ( $T > 8$  K for this sample) the field scale multiplication factor increases (approximately 30 at 10 K). The behavior in this temperature regime, however, is not consistent with the PaT hypothesis.

Our results for the nonlinear behavior of the magnetization should be contrasted with the fit to (our criterion for)  $T_G(H)$  using the “bare” de Almeida-Thouless instability criterion<sup>6</sup> [our Eq. (3)]. The field scale appears to be correct (see Figs. 5 and 6). Note, however, the steepness of the theoretical curves and the error bars in the data, the latter explicit in Fig. 6.

The nonlinear magnetization, however, seems to require an expansion of the magnetic field scale by a factor between 15 and 20 over the entire temperature range (but note the field dependence of the enhancement factor for  $T > T_G^0$ ).

This suggests the need for a “renormalization” of magnetic field coupling strength for the nonlinear portion of the magnetization, but not for the de Almeida–Thouless instability line. The former has been suggested in the literature by a number of authors.<sup>34,35</sup> It is interesting to note the satisfactory fit to the shape of the temperature ( $T > T_G^0$ ) and field dependences predicted for the nonlinear magnetization from the Sherrington-Kirkpatrick model (Figs. 7 and 8, line *a*), and using the PaT hypothesis (Fig. 8, line *b*). Thus a simple renormalization of the field

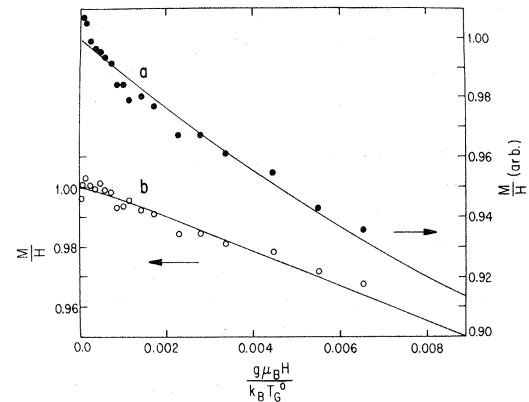


FIG. 8. The field dependence of  $M/H$  for the 2.6 at. % Ag:Mn sample at (a)  $T = 10.45$  K =  $T_G^0$  (closed symbols), and (b) at  $T = 6.5$  K ( $< T_G^0$ ) (open symbols). The solid lines are the best fits to Eqs. (5) and (6), giving  $H/J \approx 18(g\mu_B H/k_B T_G^0)$  and  $H/J = 15(g\mu_B H/k_B T_G^0)$  for (a) and (b), respectively.

appears appropriate for the nonlinear portion of the magnetization, while it does not appear necessary for the spin-glass instability line. This apparent difference in renormalization requirement may be a fruitful question for future theoretical analysis.<sup>36</sup>

## VI. CONCLUSION

From our dc magnetization results on the Ag:Mn spin-glass, we have obtained a number of characteristic temperatures associated with the spin-glass transition in the presence of a magnetic field. We have found the temperature  $T_P(H)$  to be consistent with a parameterless fit to the theoretical  $T_G(H)$  originally proposed by de Almeida and Thouless.<sup>6</sup> However, the experimental nonlinear field dependences above and below  $T_G$  we have associated with the infinite range Sherrington-Kirkpatrick model predictions<sup>9(a)</sup> (and the PaT hypothesis for  $T < T_G^0$ ) appear much larger than those predicted by theory. In addition, the value of the experimental crossover temperature,  $T_B(H)$ , is much larger than that which we have inferred from the theory. The theory and experiment can be reconciled if the ratio ( $h_{\text{theor}}/h_{\text{expt}} \approx 15-20$ ). Somewhat intriguingly, the mean “reversibility” temperature,  $\bar{T}(H)$ , would also fit extremely well with the theoretical  $T_G(H)$  if ( $h_{\text{theor}}/h_{\text{expt}} \approx 19$ ). We have argued, using the current theoretical concept for the energy surface of the spin-glass state in configuration space, that  $T_P(H)$ , and not  $T_R(H)$ , is the experimental manifestation of  $T_G(H)$ . Using this model we have also attempted to give a physical description of the various regions associated with the spin-glass transition in the presence of a magnetic field.

## ACKNOWLEDGMENTS

The authors gratefully acknowledge helpful conversations with Dr. S. Alexander, Dr. H. Bouchiat, Dr. R. H. Dee, Dr. A. J. van Duynveldt, Dr. M. Gabay, Dr. P. Monod, Dr. O. G. Symko, Dr. R. G. Palmer, and Dr. G. Toulouse. This work was supported in part by NSF under Grants No. DMR 78-27129 (R.V.C., M.H.), No. DMR 78-10312 (L.A.T.), and ONR Contract No. N00014-75-C-0245 (R.O.).

- \*Present address: Blackett Laboratory, Imperial College, London SW 7, England.
- †Present address: Corporate Research-Science Laboratories, Exxon Research and Engineering Company, Linden, N.J. 07036.
- <sup>1</sup>J. Mydosh, *J. Magn. Magn. Mater.* **15**, 99 (1980).
- <sup>2</sup>S. Nagata, P. H. Keesom, and H. R. Harrison, *Phys. Rev. B* **19**, 1633 (1979).
- <sup>3</sup>C. N. Guy, *J. Phys. F* **7**, 1505 (1977); **8**, 1309 (1978).
- <sup>4</sup>P. W. Anderson, in *Ill-Condensed Matter*, edited by Balian Maynard and G. Toulouse (North-Holland, Amsterdam, 1979).
- <sup>5</sup>S. F. Edwards and P. W. Anderson, *J. Phys. F* **5**, 965 (1975).
- <sup>6</sup>J. R. L. de Almeida and D. J. Thouless, *J. Phys. A* **11**, 983 (1978).
- <sup>7</sup>D. Sherrington and S. Kirkpatrick, *Phys. Rev. Lett.* **35**, 1792 (1975).
- <sup>8</sup>G. Toulouse, *J. Phys. (Paris) Lett.* **41**, L447 (1980).
- <sup>9</sup>(a) G. Toulouse and M. Gabay, *J. Phys. (Paris) Lett.* **42**, L103 (1981); (b) M. Gabay and G. Toulouse, *Phys. Rev. Lett.* **47**, 201 (1981).
- <sup>10</sup>J. Vannimenus, G. Toulouse, and G. Parisi, *J. Phys. (Paris)* **42**, 565 (1981).
- <sup>11</sup>P. Monod and H. Bouchiat, in *Disordered Systems and Localization*, edited by C. Castellani, C. DiCastro, and L. Peliti, Lecture notes in Physics (Springer-Verlag, Berlin, 1981), Vol. 149, p. 118.
- <sup>12</sup>99.999% pure Ag obtained from Cominco, Inc.; 99.99% pure Mn from Electronic Space Products, Inc.; 99.999% pure argon from Matheson Gas Products, Inc.
- <sup>13</sup>R. V. Chamberlin, M. Hardiman, and R. Orbach, *J. Appl. Phys.* **52**, 1771 (1981).
- <sup>14</sup>S.H.E. Corporation Model MFP.
- <sup>15</sup>J.-L. Tholence and R. Tournier, *J. Phys. (Paris)* **35**, C4-229 (1974); C. N. Guy, *J. Appl. Phys.* **50**, 7308 (1979).
- <sup>16</sup>A. Malozemoff and Y. Imry, *Phys. Rev. B* **24**, 489 (1981).
- <sup>17</sup>R. W. Knitter and J. S. Kouvel, *J. Magn. Magn. Mater.* **21**, L316 (1980).
- <sup>18</sup>G. Parisi and G. Toulouse, *J. Phys. (Paris) Lett.* **41**, L361 (1980).
- <sup>19</sup>I. Morgenstern and K. Binder, *J. Appl. Phys.* **52**, 1692 (1981).
- <sup>20</sup>C. A. M. Mulder, A. J. van Duynveldt, and J. Mydosh, *Phys. Rev. B* **23**, 1384 (1981).
- <sup>21</sup>E. D. Dahlberg, M. Hardiman, and J. Souletie, *J. Phys. (Paris) Lett.* **39**, L389 (1978).
- <sup>22</sup>J. S. Kouvel, *J. Phys. Chem. Solids* **24**, 795 (1963).
- <sup>23</sup>It is important to note that the high-temperature ( $T > 300$  K) value for  $\Theta$  must be used; as the temperature is reduced, the  $\Theta$  inferred from any given temperature interval is reduced until  $\Theta \approx 0$  in the region  $T_G < T < 2T_G$ . Some particularly clear examples of this are given in A. F. S. Morgownik and J. A. Mydosh, *Phys. Rev. B* **24**, 5277 (1981).
- <sup>24</sup>B. R. Henderson and G. V. Raynor, *J. Phys. (Paris)* **23**, 685 (1962).
- <sup>25</sup>B. R. Coles, B. V. B. Sarkissian, and R. H. Taylor, *Philos. Mag. B* **37**, 489 (1978); B. H. Verbeek and J. A. Mydosh, *J. Phys. F* **8**, L109 (1978); S. Crane and H. Claus, *Solid State Commun.* **35**, 461 (1980).
- <sup>26</sup>A. R. Kaufmann, S. T. Pan, and J. R. Clark, *Rev. Mod. Phys.* **17**, 87 (1945).
- <sup>27</sup>V. Cannella and J. Mydosh, *Phys. Rev. B* **6**, 4220 (1972).
- <sup>28</sup>E. D. Dahlberg, Ph.D. thesis (University of California, 1978) (unpublished).
- <sup>29</sup>This is the temperature associated with the line  $H_p(T)$ , in Fig. 5 of Ref. 10.
- <sup>30</sup>W. E. Fogle, J. D. Boyer, N. E. Phillips, and J. van Curen, *Phys. Rev. Lett.* **47**, 352 (1981).
- <sup>31</sup>L. R. Walker and R. E. Walstedt, *Phys. Rev. B* **22**, 3816 (1980).
- <sup>32</sup>F. T. Bantilan, Jr., and R. G. Palmer, *J. Phys. F* **11**, 261 (1981).
- <sup>33</sup>D. Fields, L. Krusin-Elbaum, and S. J. Williamson, *Bull. Am. Phys. Soc.* **25**, 176 (1980).
- <sup>34</sup>K. Binder, in *Fundamental Problems in Statistical Mechanics V*, edited by E. G. D. Cohen (North-Holland, Amsterdam, 1981).
- <sup>35</sup>R. W. Walstedt and L. R. Walker, *Phys. Rev. Lett.* **47**, 1624 (1981).
- <sup>36</sup>Suggested by G. Toulouse.